

United States Nuclear Regulatory Commission Official Hearing Exhibit	
In the Matter of:	Entergy Nuclear Operations, Inc. (Indian Point Nuclear Generating Units 2 and 3)
	ASLBP #: 07-858-03-LR-BD01
	Docket #: 05000247   05000286
	Exhibit #: RIV000051-00-BD01
	Admitted: 10/15/2012
	Rejected:
Other:	Identified: 10/15/2012
	Withdrawn:
	Stricken:



Journal of  
**Mechanical  
Science and  
Technology**

Journal of Mechanical Science and Technology 22 (2008) 2218–2227

www.springerlink.com/content/1738-494x  
DOI 10.1007/s12206-008-0912-9

## Thermal fatigue estimation due to thermal stratification in the RCS branch line using one-way FSI scheme<sup>†</sup>

Kwang-Chu Kim<sup>1</sup>, Jong-Han Lim<sup>2</sup> and Jun-Kyu Yoon<sup>2,\*</sup>

<sup>1</sup>Korea Power Engineering Company, Inc., Yongin, Gyeonggi, Republic of Korea

<sup>2</sup>Department of Mechanical & Automotive Engineering, Kyungwon University, Seongnam, Gyeonggi, Republic of Korea

(Manuscript Received June 26, 2007; Revised April 15, 2008; Accepted September 12, 2008)

### Abstract

The scheme and procedure for thermal fatigue estimation of a thermally stratified branch line were developed. One-way FSI (fluid and structure interaction) scheme was applied to evaluate the thermal stratification piping. Thermal flow analysis, stress analysis and fatigue estimation were performed in serial order. Finally, detailed monitoring locations and mitigation scheme for the integrity maintenance of piping were recommended. All wall mesh and transient temperature distribution data obtained from the CFD (computational fluid dynamics) analysis were directly imported into the input data of stress analysis model without any calculation for heat transfer coefficients. Cumulated usage factors for fatigue effect review with nodes were calculated. A modified method that combines ASME Section III, NB-3600 with NB-3200 was used because the previous method cannot consider the thermal stratification stress intensity. As the results of evaluation, the SCS (shutdown cooling system) line, branch piping of the RCS (reactor coolant system) line, shows that the CUF (cumulative usage factor) value exceeds 1.0, ASME Code limit, in case thermal stratification load is included. The HPSI (high pressure safety injection) line, re-branch piping, shows that temperature difference between top and bottom of piping exceeds the criterion temperature, 28 °C, and that the CUF value exceeds 1.0. Therefore, these branch pipings require a detailed review, monitoring or analysis. In particular, it is recommended that the HPSI piping should be shifted backward to decrease the influence of turbulent penetration intensity from the RCS piping.

*Keywords:* Thermal stratification; Thermal fatigue estimation; RCS branch line; FSI scheme

### 1. Introduction

As more experience is accumulated in the operation of existing power plants, the long-term effects of thermal hydraulic phenomena, unaccounted for in the original designs, are being observed. [1-5] One of these effects is the thermal stratification phenomenon. Thermal stratification is flow that is stabilized with temperature layers due to the density difference between hot and cold water. [6, 7] This thermal stratification in piping is capable of causing bending stress, a

serious deformation in piping, and support damage. Especially, periodic thermal stratification is capable of causing the thermal fatigue cracking of piping. [8-11]

In 1987 and 1988, thermal fatigue cracking and leakage in several PWR (pressurized water reactor) plants resulted in the issuance of NRC Bulletin 88-08. [10] In 1995, leakage from a drain line in the TMI-1 plant was attributed to the effects of turbulence penetration into the nominally stagnant uninsulated line. Similar thermal cycling incidents have continued to occur in other plants, including Tihange-1 and Dampierre-1, among others. [12, 13] In 1997, leakage from an HPI (high pressure injection)/Makeup line at Oconee increased the awareness of the NRC (Nuclear Regulatory Commission) that there were continued occurrences of thermal fatigue in small-diameter RCS

<sup>†</sup> This paper was recommended for publication in revised form by Associate Editor Jae Young Lee

\*Corresponding author. Tel.: +82 31 750 5651, Fax.: +82 31 750 5651

E-mail address: jkymoon@kyungwon.ac.kr

© KSME & Springer 2008

(reactor coolant system)-attached piping. In early 1998, there were discussions between the nuclear industry and the NRC regarding the need for additional volumetric examination of Class 1 high-pressure safety injection piping.

Several investigations have attempted to identify thermal fatigue mechanisms and to develop tools to assess piping susceptibility to thermal fatigue effects. The thermal stratification, cycling, and stripping (TASCS) program identified several critical parameters and offered predictive tools to assist in assessing fatigue loadings for thermal-structural analysis. [6] Other studies pursued experimental investigation into the thermal cycling phenomena based on scaled experiments [14–18] or full-scale plant operation. [19] Most notably, it has been shown that a swirling, vortical flow structure, as opposed to turbulence penetration, can be established in a dead-ended branch line due to the flow in the RCS line. [14, 17]

In this study, thermal fatigue estimation due to thermal stratification in the RCS branch line of KSNPP (Korea Standard Nuclear Power Plant) is performed using one-way FSI (fluid and structure interaction) scheme. Detailed thermal loading due to thermal stratification and cycling is evaluated based on temperature distributions with time, which is calculated by the CFD analysis. Fatigue effects are conservatively estimated by a modified method that combines ASME NB-3600 with NB-3200. Finally, detailed inspection locations and mitigation schemes for the integrity maintenance of piping are recommended.

## 2. Estimation schemes

### 2.1 Estimation model description

Schematic diagram for the SCS (shutdown cooling system) piping branched to RCS piping is shown in Fig. 1.

The SCS of a nuclear power plant takes charge of continually removing heat when the reactor shutdown occurs. All valves in the SCS piping are isolated during normal or startup operating condition. Also, turbulent penetration in that the higher temperature coolant out of the RCS piping penetrates into the SCS piping that is stagnant occurs. In Fig. 1, the RCS hot-leg that the higher temperature coolant passes is piping with inner diameter of 1.07 m. The SCS piping concerned in this study is piping that the nominal diameter is 0.406 m and the schedule is 160. Also, the SCS

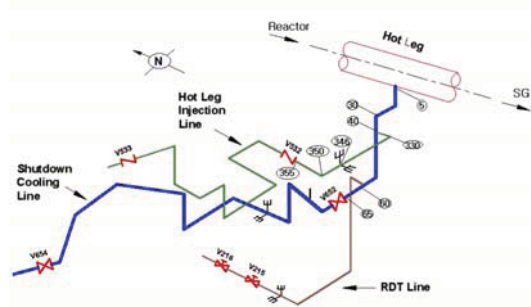


Fig. 1. Schematic diagram of the branch lines connected to the RCS piping.

piping has hot-leg HPSI (high pressure safety injection) piping and the RDT (reactor drain tank) piping. Nominal diameter of the HPSI piping is 0.076 m and nominal diameter of the RDT piping is 0.051 m.

### 2.2 Estimation procedure

In this study, a one-way FSI scheme is applied to evaluate the thermal stratification piping. Fig. 2 shows this estimation procedure performed by using the one-way FSI scheme. First, geometry and mesh for numerical analysis is generated. Next, thermal flow analysis on thermal stratification piping is performed by the CFD code. Temperature difference between top and bottom of piping is compared with the criterion temperature, 28°C (50°F) stated in reference. [6, 10, 11] The only solid region except the fluid region out of the CFD results is transferred into the stress analysis. At this time, geometry, mesh and temperature distribution data of solid region are converted into input data format for stress analysis by some user's operation for MpCCI (mesh-based parallel code coupling interface) between CFD code and CSD (computational structure dynamics) code. A special MpCCI code was not used. Therefore, all wall mesh and temperature distribution data with time were directly imported into the input data of stress analysis model without any calculation for heat transfer coefficients. This scheme is different from previous studies which use the average heat transfer coefficients of wall surface in stress analysis and it is more realistic. Fatigue effects are estimated by a modified method that combines ASME NB-3600 with NB-3200. This is to reflect the thermal stratification load to the existing design stress. Finally, detailed monitoring locations and mitigation schemes for the integrity maintenance of piping are recommended.

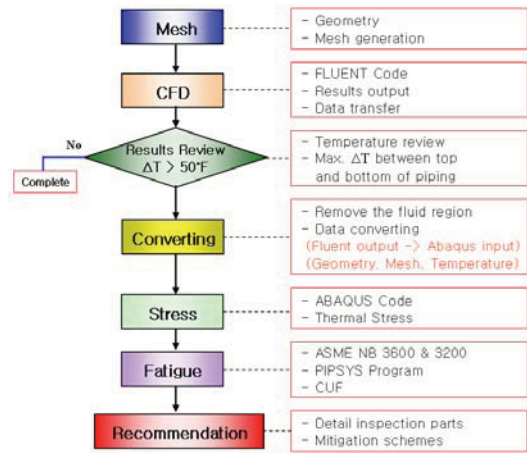


Fig. 2. Estimation procedure using one-way FSI scheme.

### 3. Numerical analysis

#### 3.1 Governing equations

For the FSI evaluation, governing equations for thermal flow and structure are needed. In this study, unsteady, incompressible and three-dimensional conservation equations are used as governing equations for the thermal flow analysis. Stress equilibrium equation is used for the stress analysis. Standard k-ε model is used for turbulent model and Boussinesq's approximation is used for the buoyancy effects. Assuming that all properties are constant under given temperature and pressure, the governing equations used are as follows:

##### Continuity equation

$$\frac{\partial}{\partial x_i}(\rho u_i) = 0 \quad (1)$$

##### Momentum Equation

$$\begin{aligned} \frac{\partial}{\partial x_j}(\rho u_j u_i) &= -\frac{\partial p}{\partial x_i} + \rho g_i \beta (T - T_{cold}) \\ &+ \frac{\partial}{\partial x_j} \left[ (\mu + \mu_t) \left( \frac{\partial u_i}{\partial x_j} + \frac{\partial u_j}{\partial x_i} \right) - \frac{2}{3} k \delta_{ij} \right] \end{aligned} \quad (2)$$

##### Turbulent equation (standard k-ε)

$$\begin{aligned} \frac{\partial}{\partial x_j}(\rho u_j k) &= \frac{\partial}{\partial x_j} \left[ \left( \mu + \frac{\mu_t}{\sigma_k} \right) \frac{\partial k}{\partial x_j} \right] \\ &+ P_k + G_b - \rho \epsilon \end{aligned} \quad (3)$$

$$\begin{aligned} \frac{\partial}{\partial x_j}(\rho u_j \epsilon) &= \frac{\partial}{\partial x_j} \left[ \left( \mu + \frac{\mu_t}{\sigma_\epsilon} \right) \frac{\partial \epsilon}{\partial x_j} \right] \\ &+ \frac{\epsilon}{k} [C_1 (P_k + G_b) - C_2 \rho \epsilon] \end{aligned} \quad (4)$$

##### Stress equilibrium equation

$$\frac{\partial \sigma_{ij}}{\partial x_i} + b_j = 0 \quad (5)$$

where,  $b_j$  is external force.

##### Energy equation

$$\frac{\partial}{\partial x_j}(\rho u_j T) = \frac{\partial}{\partial x_j} \left\{ \left( \frac{\mu_t}{\sigma_t} + \frac{k_f}{C_p} \right) \frac{\partial T}{\partial x_j} \right\} \quad (6)$$

where, the coefficient, source term, and turbulent constants are as follows:

$$\mu_t = \rho C_\mu k^2 / \epsilon$$

$$P_k = \mu_t \left( \frac{\partial u_i}{\partial x_j} + \frac{\partial u_j}{\partial x_i} \right) \frac{\partial u_i}{\partial x_j}$$

$$G_b = -\frac{\mu_t}{\sigma_t} g_i \beta \frac{\partial T}{\partial x_i}$$

$$\sigma_t = 0.85, \sigma_k = 1.0, \sigma_\epsilon = 1.3, C_\mu = 0.09,$$

$$C_1 = 1.44, C_2 = 1.92$$

#### 3.2 Numerical schemes

The FLUENT code [20] based on finite volume method is used for the CFD analysis. The ABAQUS code [21] based on the finite element method is used for stress analysis. Finally, fatigue estimation is performed by the PIPSIS program. [22] The grid system for CFD analysis is shown in Fig. 3. The number of cells is 87,776. The length from the connection point of the RCS piping with the SCS piping to the outlet of the RCS hot-leg is assumed to be more than 20 times the SCS piping diameter to reflect on flow change in the connection part and to improve convergence. The range of analysis for the SCS piping, for the HPSI piping, and for the RDT piping is set to the extent of suitable length passing the 1<sup>st</sup> valve in consideration of thermal stratification effect and support position.

The SIMPLE (semi-implicit method for pressure linked equations) algorithm is used to calculate the pressure field at each cell. [23] Upwind scheme is

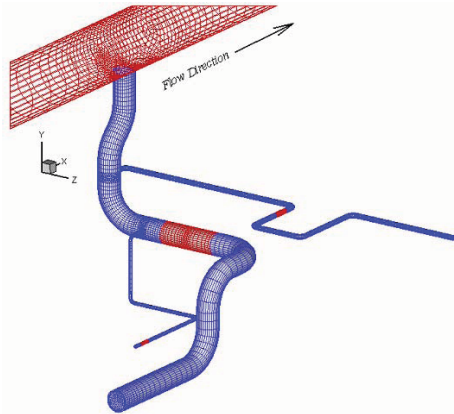


Fig. 3. Grid systems for the numerical analysis.

used to determine the convection term. The convergence criterion is that the residual is less than  $1.0 \times 10^{-5}$  at the each time step. To satisfy this convergence criterion, iterations of less than 50 times per time step of 1 second are needed. Unsteady CFD calculation is performed until 3000 second. To improve the convergence, under-relaxation factors are applied. Computer time for only CFD calculation took about 16 days using the Pentium 2.0 GHz.

In this study, thermal stripping of the temperature layer in the fluid region and two-way FSI scheme are ignored. To simulate the stripping, a high turbulent model like LES model is needed. However, this high turbulent model and two-way FSI method demand too much more time and the problem is difficult to solve actually.

### 3.3 Boundary conditions

Temperature and flow rate of coolant in inlet of the RCS hot-leg are  $327^\circ\text{C}$  and  $7718 \text{ kg/s}$ , respectively. Inlet turbulent intensity is assumed to be 10 percent for hydraulic diameter. Outlet boundary condition is the constant pressure condition. All outer surfaces of piping including the RCS piping are assumed to be adiabatic wall. All valves in the SCS piping, the HPSI piping and the RDT piping are assumed to be isolated. There is no leakage throughout valve disks. The disk thickness in valves is assumed to be as two times as piping thickness. Each end surface of branch piping in the range of analysis is assumed to be isolated and to be a low temperature wall of  $49^\circ\text{C}$ . In the process of numerical calculation, the initial temperature condition is set to be  $49^\circ\text{C}$ . The values for condition of average temperature in

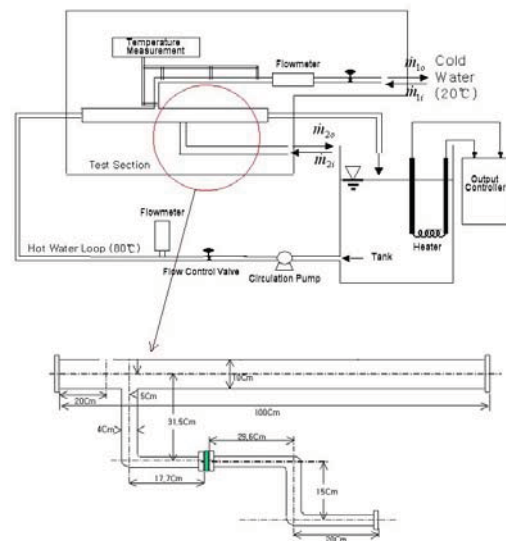


Fig. 4. Experiment schematic for verification of numerical schemes.

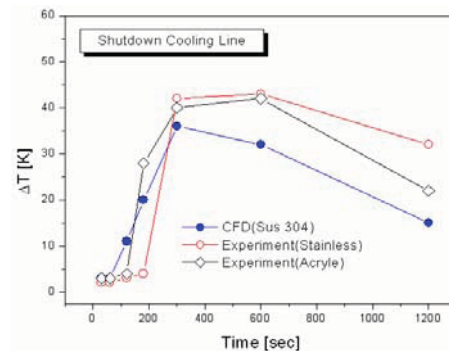


Fig. 5. The comparison of CFD results with experimental results.

15.5 MPa are used for the properties of fluid. The material of solid is assumed to be SUS304.

### 3.4 Experimental verification

To verify the numerical schemes used in this analysis, a simplified experiment with one branch line as shown in Fig. 4 was performed at small scale. [18] Hot water temperature and flow rate of the main piping were  $80^\circ\text{C}$  and  $4.65 \text{ kg/s}$  and cold water temperature was  $20^\circ\text{C}$ . CFD calculation for comparison with experimental results was performed with the same schemes (the number of meshes, turbulent model, algorithm and so on) mentioned in session 3.2. Fig. 5 shows a comparison of the CFD result

with the experimental result. There is some difference in accuracy but the trend is similar. Therefore, numerical schemes adopted in this study are considered to be suitable because the purpose of this estimation is to look for the detailed monitoring location and mitigation scheme for the integrity maintenance of piping, and because much mesh and high turbulent model demand too much time and are capable of generating unstable convergence.

## 4. Results and discussions

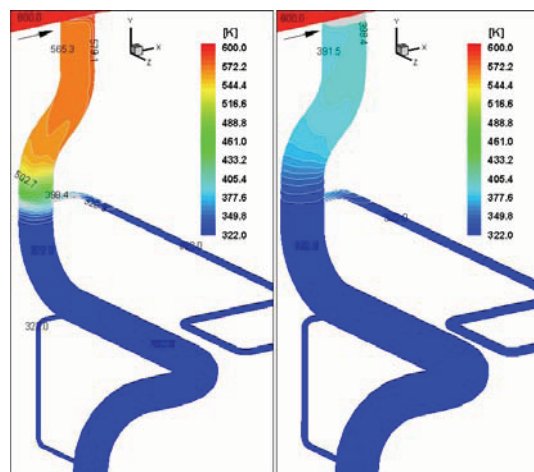
### 4.1 Thermal flow analysis

To evaluate the temperature distributions for the SCS, HPSI and RDT lines due to the turbulent penetration, a transient 3-dimensional numerical thermal hydraulic analysis was performed by the CFD code, FLUENT.

Fig. 6 to Fig. 7 shows the temperature distributions with time in the SCS piping including the HPSI piping and the RDT piping. Turbulence occurs

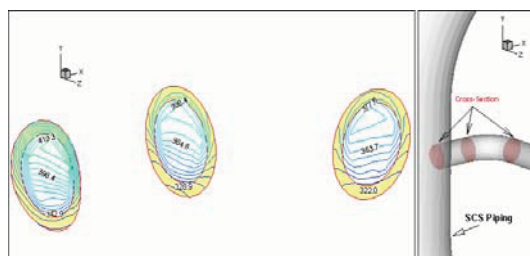
when the main flow in the RCS line creates a secondary flow in a branch line. Length of turbulent penetration in branch line depends on the velocity and temperature of the RCS flow. This turbulent penetration mainly occurs during plant heat-up and cool-down operations and becomes the source of thermal stratification. [6, 19, 24, 25] Fig. 6 shows the temperature distribution at 100 sec. Turbulence penetrates rapidly into the SCS piping from the RCS piping; therefore, a thermal stratification effect in the horizontal piping of the HPSI line appears due to the turbulent penetration from the SCS piping. At the beginning of penetration, the fast inflow from the RCS piping generates a higher temperature for the inner wall than the outer wall in the SCS piping.

Fig. 7 shows the temperature distribution at 500 sec. Thermal stratification phenomenon is shown in the horizontal part of the SCS piping. However, this effect in the HPSI piping was largely decreased despite continuous penetration. This is judged to result from a strong thermal mixing effect as the piping diameter is

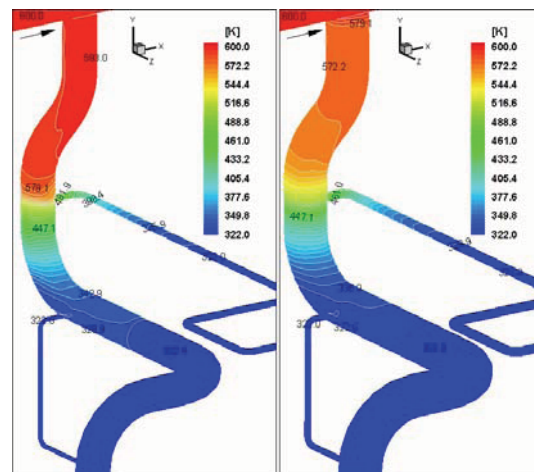


(a) Inner wall

(b) Outer wall

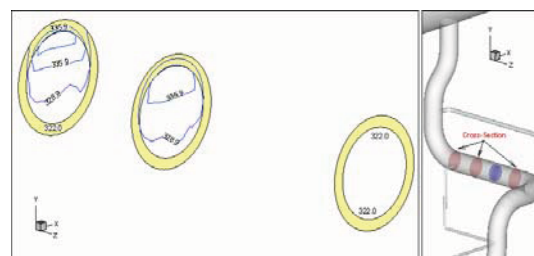


(c) Detail contour in cross sectional area



(a) Inner wall

(b) Outer wall



(c) Detail contour in cross sectional area

Fig. 6. Temperature distributions with time in branch lines ( $t=100$  sec).

Fig. 7. Temperature distributions with time in branch lines ( $t=500$  sec).

small.

Fig. 8 shows measurement positions for temperature difference review. Nine positions were totally investigated.

Fig. 9 represents the temperature changes with time at point 1 in the vertical piping of the SCS piping that is near the RCS piping. Four points that were located at intervals of  $90^\circ$  in the cross-sectional area were examined. At the beginning of turbulent penetration from the RCS piping, each point has a different temperature due to the flow direction and the difference of penetration intensity. However, the temperature difference is rapidly decreased as time passes, and the temperature values at all points begin to be similar after 400 sec.

Fig. 10 shows the temperature difference changes between top and bottom inner wall at point 3 with time. Point 3 is located at the starting point of the horizontal piping passing the 1<sup>st</sup> elbow of the SCS piping. The maximum temperature difference of

$19.4^\circ\text{C}$  is observed at 500 sec and the temperature difference is decreased after 500 sec.

Fig. 11 represents the temperature difference changes between top and bottom inner wall at the points 5, 6 and 7 with time. The points 5 to 7 are located in the horizontal part of the HPSI piping connected with the SCS piping. As all points are directly affected by turbulent penetration from the SCS piping, a severe temperature difference is shown that exceeds the criterion temperature,  $28^\circ\text{C}$ .

Fig. 12 represents the temperature difference changes between top and bottom inner wall at point 8 with time. This point is located in the horizontal piping of the RDT piping connected with the SCS piping. A temperature difference appears but is tiny. It is judged that this result is because the drain piping is located backward compared with the HPSI piping and the magnitude of turbulent penetration from the SCS piping is only slight.

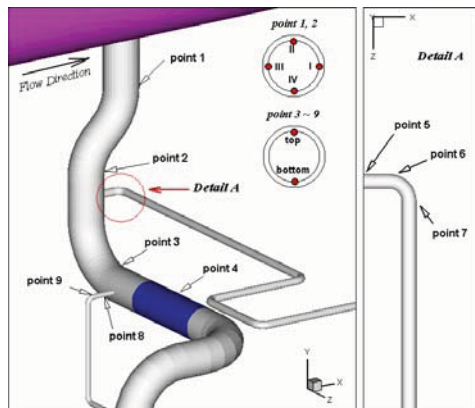


Fig. 8. Schematic diagram of the positions for temperature measurement.

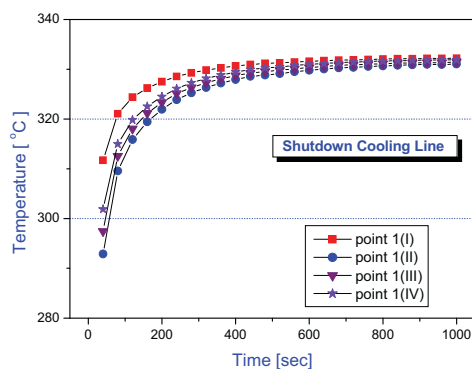


Fig. 9. Temperature changes with time at point 1.

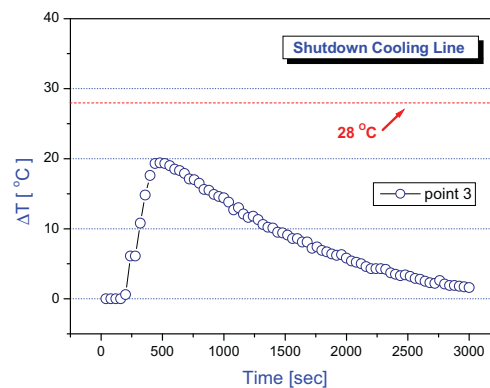


Fig. 10. Temperature changes with time at point 3.

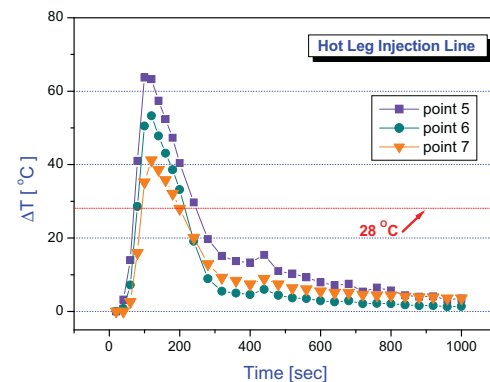


Fig. 11. Temperature changes with time at points 5, 6 and 7.

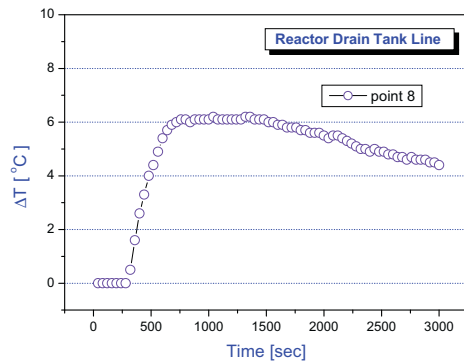


Fig. 12. Temperature changes with time at point 8.

#### 4.2 Stress/fatigue analysis

All wall temperature distribution and mesh data with time were directly imported into the input data of stress analysis model without any calculation for heat transfer coefficients. Thermal stress loads due to the turbulent penetration were analyzed by the FEM code, ABAQUS.

For each node location as shown in Fig. 1, thermal stratification stress intensity,  $S_{T/S}$ , is indicated in Table 1. As only thermal load was considered, therefore, pressure and moment loads should be included in the peak stress to evaluate the fatigue effects of each line. To include thermal stratification stress intensity, a modified peak stress intensity range,  $S_p^*$ , was calculated as follows:

$$S_p^* = S_p + S_{T/S} \quad (7)$$

where,  $S_p$  is a design peak stress intensity that is calculated by Eq. 11 of ASME Section III, NB-3653.2, and  $S_{T/S}$  is a thermal stratification stress intensity that is calculated by NB-3215.

Using the PIPSYS program, which is the piping design program of KSNPP, alternating stress intensity,  $S_{alts}$ , was calculated by NB-3653.3 or NB-3653.6 and the cumulative usage factors (CUF) were evaluated by NB-3653.4 and NB-3653.5.

For each node location as shown in Fig. 1, design CUF and revised CUF are summarized in Table 2. The CUF of node 40, where a tee junction is connected between the SCS piping and HPSI piping, was increased suddenly because of thermal stratification in the HPSI piping due to the secondary turbulent penetration. Also, the CUF of node 60, where a tee junction is connected between the SCS piping and RDT piping, was increased. The increase of the CUF

Table 1. Thermal stratification stress intensities.

Line	No. of Node	Location	$S_{T/S}$ (MPa)
Shutdown Cooling	5	Weldment of Nozzle	401.7
	30	90 Elbow	370.7
	40	Tee Junction	394.8
	60	Tee Junction	82.7
	65	Weldment of Valve	118.5
Hot Leg Safety Injection	330	90 Elbow	89.6
	346	Support	39.3
	350	90 Elbow	21.4
	355	Weldment of Valve	14.5

Table 2. Cumulated usage factors (CUF).

Line	No. of Node	Design CUF	$S_p^*$ (MPa)	Revised CUF
Shutdown Cooling	5	0.337	1166.5	0.461
	30	0.488	1156.1	0.631
	40	0.818	2744.3	1.229
	60	0.719	2818.0	1.000
	65	0.228	842.0	0.228
Hot Leg Safety Injection	330	0.155	737.2	0.155
	346	0.097	785.5	0.099
	350	0.153	769.6	0.153
	355	<0.001	223.2	<0.001

at other locations was insignificant to maintain the fatigue integrity.

#### 4.3 Recommendations

In branch layout lines that the CUF is shown highly in this study, it is recommended that for these parts for a fully detailed stress analysis should be performed or should be managed in the minimum using enhanced inspection or monitoring for possible fatigue failure or leakage.

In particular, a scheme to mitigate the thermal stratification effect in the HPSI piping should be considered. Fig. 13 is a schematic diagram suggested to mitigate the thermal stratification effect in the HPSI piping. To minimize the calculation time, the layout of the SCS and the HPSI lines was simplified and the RDT line was excluded. Fig. 14 shows temperature difference in the HPSI piping compared to the case connected to vertical piping of the SCS line with the case connected to horizontal piping of the SCS line. Temperature difference of the case connected

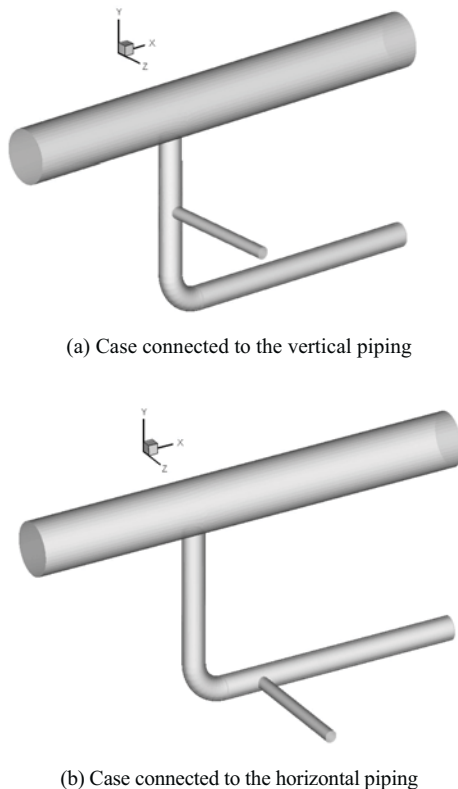


Fig. 13. Schematic diagram suggested to mitigate the thermal stratification effect of HPSI line.

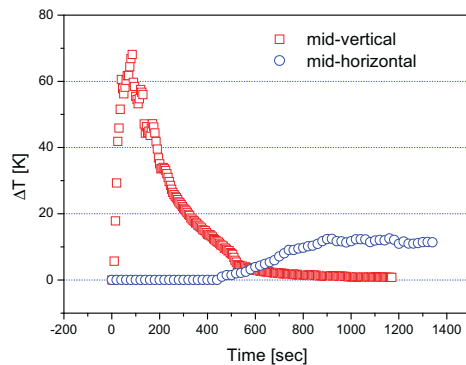


Fig. 14. Temperature difference change in the HPSI piping compared the case connected to vertical piping of SCS line with the case connected to horizontal piping of SCS line.

to horizontal piping is lower than that of the case connected to vertical piping. Thus, it is recommended that HPSI piping should be shifted backward to decrease the influence of turbulent penetration intensity from the RCS piping.

## 5. Conclusions

A thermal fatigue estimation scheme for a thermally stratified branch line that has re-branch line was developed. Generally, the thermal stratification effect of re-branched lines has not been considered in the fatigue evaluation for plant design. In this study, a one-way FSI scheme is used to evaluate the thermal stratification piping. Thermal flow analysis, stress analysis and fatigue estimation were performed in serial order. Finally, detailed monitoring locations and mitigation scheme for the integrity maintenance of piping were recommended. All wall mesh and transient temperature distribution data obtained in the CFD analysis were directly imported into the input data of stress analysis model without any calculation for heat transfer coefficients. This scheme is different from the previous studies which have used the average heat transfer coefficients of wall surface in stress analysis and is more realistic.

The CUF, cumulated usage factors, for fatigue effect review with node were calculated. A modified method that combines ASME NB-3600 with NB-3200 was used. This is because the previous estimation method uses just the ASME Section III, NB-3600 that cannot consider the thermal stratification stress intensity. Thermal stratification stress intensity is obtained from ASME Section III, NB-3200. Modified peak stress includes thermal stratification stress intensity to design peak stress intensity obtained from ASME Section III, NB-3600.

In this study, the SCS line, branch piping of the RCS line, shows that the CUF value exceeds 1.0, ASME Code limit, in case thermal stratification load is included. The HPSI line, re-branch piping, shows that the temperature difference between top and bottom of piping exceeds the criterion temperature, 28 °C and that the CUF value exceeds 1.0. Therefore, on these branch lines, a detailed review, monitoring or analysis is required. In particular, it is recommended that the HPSI piping should be shifted backward to decrease the influence of turbulent penetration intensity from the RCS piping.

Thermal stripping and two-way FSI method were ignored in this study, but these can be possible if an economical high turbulence model and rapid computer is developed. Therefore, further study on these is required.

## References

- [1] Boulder, Co., *Nuclear Power Experience (NPE)*, Published by RCG/Hagler, Bailly, Inc., (1993).
- [2] Framatome, *RHRS Elbow Cracking at Civaux 1*, Significant Event Report No. 14, (1988).
- [3] Hagki Youm, et al., Numerical Analysis for Unsteady Thermal Stratified Turbulent Flow in a Horizontal Circular Cylinder, *ICONE-4 Conference*, (1996).
- [4] Hagki Youm, et al., Development of Numerical Analysis Model for Thermal Mixing in the Reactor Pressure Vessel, *ASME, PVP-2000 Conference*, (2000).
- [5] KEPRI & KOPEC, *Pressurized Thermal Shock Evaluation for Reactor Pressure Vessel of Kori Unit 1*, Technical Report-TR.96BJ12.J1999.81, (1999).
- [6] EPRI, *Thermal Stratification, Cycling and Striping (TASCS)*, TR-103581, (1994).
- [7] D. H. Roarty, P. L. Strauch and J. H. Kim, Thermal Stratification, Cycling and Striping Evaluation Methodology, Changing Priorities of Codes and Standards: Failure, Fatigue, and Creep, ed. K. R. Rao and J. A. Todd, *J. of ASME PVP*,. 286, (1994) 49-54.
- [8] EPRI, *Operating Experience Regarding Thermal Fatigue of Unisolable Piping Connected to PWR Reactor Coolant Systems (MPR-25)*, TR-1001006, (2000).
- [9] NRC, *Cracking in Feedwater System Piping*, Bulletin No. 79-13, (1979).
- [10] NRC, *Thermal Stresses in Piping Connected to Reactor Coolant Systems*, Bulletin 88-08, (1988).
- [11] NRC, *Pressurizer Surge Line Thermal Stratification*, Bulletin No. 88-11, (1988).
- [12] OECD NEA, *Thermal Cycling in LWR components in OECD-NEA member countries*, (2005).
- [13] R. Magee, et al., *J. M. Farley Unit 2 Engineering Evaluation of the Weld Joint Crack in the 6" SI/RHR piping*, WCAP-11789, (1988).
- [14] M. Robert, Corkscrew Flow Pattern in Piping System Dead Legs, *NURETH-5 Conferenc*, (1992).
- [15] N. Nakamori, K. Hanzawa, T. Ueno, J. Kasahara, and S. Shirahama, Research on Thermal Stratification in Un-isolable Piping of Reactor Coolant Pressure Boundary', Experience with Thermal Fatigue in LWR Piping Caused by Mixing and Stratification, *Specialist Meeting Proceedings*, (1998).
- [16] R. M. Roidt and J. H. Kim, Analytical and Experimental Studies of a Stratified Flow in a Pipe, *NURETH-6 Conference*, France, October 5-8, 1, (1993) 541-547.
- [17] J. H. Kim, R. M. Roidt and A. F. Deardorff, Thermal Stratification and Reactor Piping Integrity, *Nuclear Engineering and Design*, 139, No. 1, (1993) 83-96.
- [18] S. N. Kim, S. H. Hwang and K. H. Yoon, *Journal of Mechanical Science and Technology*, 9, No. 5, (2005) 1206-1215.
- [19] EPRI, *EDF Thermal Fatigue Monitoring Experience on Reactor Coolant System Auxiliary Piping (MRP-69)*, TR-1003082, (2001).
- [20] *FLUENT User's Guide*, Fluent Inc., (1998).
- [21] *ABAQUS Standard User's Manual*, Hibbitt, Karlsson & Sorensen, Inc.: Pawtucket, (1998).
- [22] S&L, *Integrated Piping Analysis System*, S&L Program No. 303.7.026-2.2, (1995).
- [23] S. V. Partankar, *Numerical Heat Transfer and Fluid Flow*, McGraw-Hill Book Company, (1980).
- [24] M. H. Park and K. C. Kim, Thermal stratification phenomenon and evaluation in piping, *Piping Journal*, 18, No. 6, (2004) 188-191.
- [25] M. H. Park and K. C. Kim, Thermal stratification phenomenon and evaluation in piping, *Piping Journal*, 18, No. 7, (2004) 206-209.



**Kwang-Chu Kim** received his B.S., M.S. and Ph.D degrees from department of mechanical engineering, Kyunghee University in 1993, 1995 and 2000, respectively. He has worked for Korea Power Engineering Company since 1995 and he is now a senior researcher. Dr. Kim's research area includes CFD analysis, flow control, plant design and simulator.



**Jong-Han Lim** received his B.S. degree from department of mechanical engineering, Chosun University in 1981, M.S. and Ph.D degrees from department of mechanical engineering, Kyunghee University in 1986 and 1992, respectively. He worked for Hyundai Motors Company during 1986-

95. He is now a professor in department of mechanical & automotive engineering, Kyungwon University. Dr. Lim's research interests are in the area of thermal flow, internal combustion and liquid atomization.



**Jun-Kyu Yoon** received his B.S. degree from department of mechanical engineering, Chosun University in 1981, M.S. degree from department of mechanical engineering, Kyunghee University in 1987 and Ph.D degree from department of mechanical engineering, Myongji University in 2001. He worked for Hyundai Motors Company and Asia Motors Company during 1985-96. He is now a professor in department of mechanical & automotive engineering, Kyungwon University. Dr. Yoon's research interests are in the area of flow control, heat transfer, liquid atomization, spray and combustion.